Coupled electron spin resonance of non-S-state impurities in metals

S. A. Dodds* and T. Plefka†
Physics Department, University of California, Los Angeles, California 90024
(Received 10 November 1976; revised manuscript received 9 February 1978)

The dynamical coupling of the individual crystal-field transitions and the conduction electrons is investigated for non-S-state ions in an arbitrary crystal field. The equations given are the result of a microscopic quantum-statistical treatment. All relevant terms of the transition matrix have been calculated in the lowest nonvanishing order of perturbation theory. The results allow a quantitative description of the experimental ESR spectra. A particular physically realistic example is discussed in detail. A large temperature-dependent g shift and a decrease of the width with increasing concentration is found for the local-moment resonance. At high temperatures the coupling to the excited states plays an important role and in particular affects the conduction-electron resonance shift. The relevance of these effects for actual physical situations is discussed in some detail.

I. INTRODUCTION

The electron spin resonance (ESR) of localized magnetic impurities has been studied in detail during the last several years. (For an excellent general review see Ref. 1, and for an experimental review see Ref. 2.) Both S-state and non-S-state ions have been investigated. It has been well known, since the paper of Hasegawa,[3] that for S-state ions the coupling between the conduction electrons and the local moment magnetization is very important, leading to the "bottleneck" effects. Non-S-state impurities are believed to be less sensitive to this dynamic coupling because of the usually large difference in the g values (see, e.g., Ref. 1). If the coupling can be neglected, then the localized moment resonance frequency is changed by the Knight shift and the conduction-electron frequency by the "Day" shift. The widths of the resonances are given by the Korringa and the Overhauser rates, respectively. The usual S-state expressions[1,3] for these quantities must be modified in the presence of a crystal field, and this was done in Refs. 4 and 5.

There are situations, even for non-S-state ions, where the coupling may become important. Since the Overhauser rate is very rapid at higher concentration,[6] coupling effects will occur because the resonance lines overlap. A second case where the coupling for non-S-state ions will be important arises at high temperatures, as pointed out in Ref. 5. Even if the ground-state resonance of the local moments is too far away for coupling to occur, effects due to the coupling to transitions within the excited levels can become important. A detailed knowledge of these effects is very important for transmission ESR experiments,[5] since one deduces crystal-field parameters from the temperature dependence of the conduction electron spin resonance (CESR) shift and width.

To study these effects quantitatively, a full set of equations for the dynamics of the conduction-electron magnetization coupled to all possible crystal-field transitions is needed. Fortunately, there exists a theory for the analogous problem for S-state ions, developed independently by Barnes[7] and by one of the authors,[8] and successfully applied for the interpretation of the experimental data.[9,10] In Sec. II we will generalize the treatment of Ref. 8 for an arbitrary crystal field. The results of this theory will be discussed for a particular example in Sec III. Finally, in Sec. IV, we will point out the relevance of the coupling effects in actual physical situations.

II. COUPLED RESONANCE EQUATIONS

As the theoretical problem is similar to the problem for S-state ions, which has been worked out in detail,[7,8] we shall present here only the changes in the ansatz and shall try to make the reader familiar with the results. The same Hamiltonian as in Ref. 8 is used, except that the spin operators $\vec{S}$ are replaced by the total angular momentum $\vec{J}$ and we use different g values for the conduction electrons and the local moments, respectively, g_s and the Landé factor g_J. The $2J+1$ single-ion energy levels are denoted by ϵ_n and the corresponding states by $|n\rangle$. The energy levels are, in general, multiply degenerate in zero magnetic field. A schematic term scheme is shown in Fig. 1, in the presence of an applied field along the z direction. We assume that the Zeeman energies, $g_s\mu_B H$ and $g_J\mu_B H$, are small compared to the zero-field splittings of the isolated ions, which is the opposite limit from Ref. 8. Thus, in contrast to Ref. 8, where the selection rules allow only $\Delta M = \pm 1$ transitions, the selection

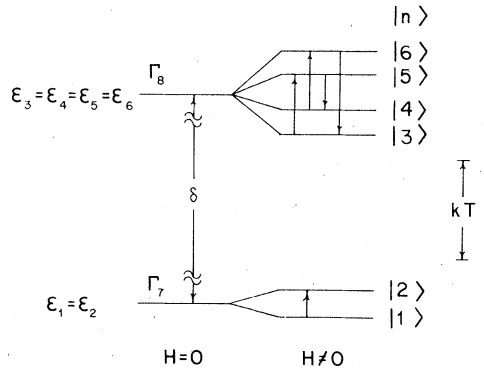

FIG. 1. Schematic single-ion level scheme with a Γ_7 ground state and a Γ_8 first excited state. The arrows indicate the possible ESR transition when a small static magnetic field is applied in the [100] direction. See Sec. III for more details.

rules here are quite weak and, in general, allow all of the transitions $n \rightarrow n'$ to occur. However, in ESR only the transitions *within* a crystal-field multiplet can be seen. For these ESR transitions, we choose the notation $\alpha \rightarrow \alpha'$ (see Fig. 1). Their actual number depends strongly on the symmetry of the particular crystal field and the direction of the external magnetic field.

The dynamics of this system may be described by a coupled set of phenomenological Bloch equations. One Bloch equation is needed for each crystal field transition $\alpha \rightarrow \alpha'$ and for the components of the conduction-electron magnetization.[11] To obtain expressions for the dynamic susceptibility $\chi^{\nu\nu'}(\omega)$ from this set of Bloch equations, one has to linearize with respect to the driving field and then perform a Fourier transformation. In the expression for $\chi^{\nu\nu'}(\omega)$ obtained in this way, phenomenological internal fields and relaxation times, introduced in the Bloch equation ansatz, remain as unknown parameters. They are usually calculated from additional considerations.

We choose instead an equivalent but more direct quantum statistical approach, for which, however, some more mathematical background is needed. We start from the Kubo formula for the dynamic susceptibility tensor $\chi^{\nu\nu'}(\omega)$, which describes the response of the $-\nu$ component of the total magnetization $\delta M^{-\nu}(t) = N\chi^{\nu\nu'} h^{-\nu'}(t)$ to a field $h^{-\nu'}(t) \sim e^{i\omega t}$ in the $-\nu$ direction. [In this work, $A^0 = A^z$ and $A^{\pm 1} = 2^{-1/2}(A^x \pm iA^y)$ are used as components of a vector $\vec{A}$.] Here, ω is the rf frequency, and N the number of conduction electrons per unit volume. As in Ref. 8, we employ Mori's[12] projector formalism[13] and obtain

$$\chi^{\nu\nu'}(\omega) = \sum_{MM'} (e_M^{\nu})^* \chi_{MM'} e_{M'}^{\nu'} - \omega \sum_{\substack{MM' \\ M''M'''}} (e_M^{\nu})^* \chi_{MM'} \Omega^{-1}_{M'M''}(\omega) \times \chi_{M''M'''} e_{M'''}^{\nu'} \ . \tag{1}$$

The index M can be $\nu = -1, 0, +1$ or $\alpha\alpha'$, representing the components of the conduction electron magnetization or the individual crystal-field transitions $\alpha \rightarrow \alpha'$, respectively. $\Omega^{-1}_{MM'}$ is the inverse of the transition matrix

$$\Omega_{M\hat{M}} = \begin{pmatrix} \Omega_{\nu,\hat{\nu}} & \Omega_{\nu,\hat{\alpha}\hat{\alpha}'} \\ \Omega_{\alpha\alpha',\hat{\nu}} & \Omega_{\alpha\alpha',\hat{\alpha}\hat{\alpha}'} \end{pmatrix} . \tag{2}$$

The $\chi_{MM'}$ are the partial static susceptibilities of our subsystems ν and $\alpha\alpha'$ and the e_M^{ν} are defined as

$$e_{\nu}^{\hat{\nu}} = \mu_B g_s \delta_{\nu\hat{\nu}} \quad \text{and} \quad e_{nn'}^{\hat{\nu}} = \mu_B g_J \langle n | J^{\hat{\nu}} | n' \rangle \ . \tag{3}$$

For the partial static susceptibilities, we use the molecular-field approximation leading to

$$\chi_{\nu,\hat{\nu}} = \chi_{\nu}^0 \left(\delta_{\nu\hat{\nu}} + 2J_{sf} \sum_{\bar{n},\bar{n}'} \langle \bar{n}' | J^{-\nu} | \bar{n} \rangle \chi_{\bar{n}\bar{n}',\hat{\nu}} \right) , \tag{4a}$$

$$\chi_{\nu,\hat{n}\hat{n}'} = 2J_{sf} \chi_{\nu}^0 \sum_{\bar{n}\bar{n}'} \langle \bar{n}' | J^{-\nu} | \bar{n} \rangle \chi_{\bar{n}\bar{n}',\hat{n}\hat{n}'} \ , \tag{4b}$$

$$\chi_{nn',\hat{\nu}} = 2J_{sf} \chi_{nn'}^0 \sum_{\bar{\nu}} \langle n | J^{\bar{\nu}} | n' \rangle \chi_{\bar{\nu},\hat{\nu}} \ , \tag{4c}$$

$$\chi_{nn',\hat{n}\hat{n}'} = \chi_{nn'}^0 \left(\delta_{n\hat{n}} \delta_{n\hat{n}'} + 2J_{sf} \sum_{\bar{\nu}} \langle n | J^{\bar{\nu}} | n' \rangle \chi_{\bar{\nu},\hat{n}\hat{n}'} \right) \ , \tag{4d}$$

from which the matrix $\chi_{MM'}$ can be calculated. J_{sf} is the coupling constant of the s-f exchange interaction, used here in the form $-2J_{sf}\delta(R_i)\vec{J}_i \cdot \vec{s}$. For temperatures $kT = 1/\beta$, large compared to the Zeeman splittings within the crystal-field multiplets, the bare static susceptibilities are given by

$$\chi_{\nu}^0 = \tfrac{1}{2}\rho_0 \ , \quad \chi_{nn'}^0 = \frac{c}{Z} \frac{\exp(-\beta\epsilon_n) - \exp(-\beta\epsilon_{n'})}{\epsilon_{n'} - \epsilon_n} \ , \tag{5}$$

where ρ_0 is the (one-spin) density of states per electron at the Fermi surface, c the impurity concentration, and $Z = \sum_n \exp(-\beta\epsilon_n)$ the partition function of a single impurity ion.

Mori's formalism gives exact expressions for the transition matrix elements

$$\Omega_{M\hat{M}}(\omega) = \omega\chi_{M\hat{M}} + L_{M\hat{M}} - i\chi_M^0 \Delta_{M\hat{M}} \ , \tag{6}$$

which, however, need further approximations. We evaluate the real part of the self-energy in perturbation theory with respect to the s-f ex-

change interaction to the lowest nonvanishing order (i.e., second order) and neglect the imaginary part.[14] The remaining contributions to the transition matrix are again calculated in molecular-field approximation. For simplicity, we restrict ourselves to temperatures high compared to the Zeeman splittings within the multiplets. We finally obtain for $L_{MM'}$

$$L_{\nu,\hat{\nu}} = -\nu\delta_{\nu\hat{\nu}}\langle s^0\rangle + \hat{\nu}\delta_{0\nu}\langle s^{\hat{\nu}}\rangle + \nu\delta_{0\hat{\nu}}\langle s^{-\nu}\rangle \,, \tag{7a}$$

$$L_{\nu,\hat{\alpha}\hat{\alpha}'} = L_{\alpha\alpha',\hat{\nu}} = 0 \,, \tag{7b}$$

$$L_{\alpha\alpha',\hat{\alpha}\hat{\alpha}'} = \sum_{n,n'} (\delta_{\alpha\hat{\alpha}}\chi_{\hat{\alpha}'\alpha';nn'} - \delta_{\alpha'\hat{\alpha}'}\chi_{\alpha\hat{\alpha},nn'})e^0_{nn'}H + (\delta_{\alpha\hat{\alpha}}\chi_{\hat{\alpha}'\alpha',0} - \delta_{\alpha'\hat{\alpha}'}\chi_{\alpha\hat{\alpha},0})\mu_B g_s H \,, \tag{7c}$$

where $\langle s^\nu\rangle$ is given by

$$\langle s^{-\nu}\rangle = \chi_{\nu,0}\mu_B g_S H + \sum_{n,n'} \chi_{\nu,nn'}e^0_{nn'}H \,. \tag{8}$$

The expressions obtained for the relaxation rates $\Delta_{MM'}$ are much more complicated

$$\Delta_{\nu,\hat{\nu}} = 4\pi J_{sf}^2\rho_0\frac{c\beta}{Z}\sum_{n,n'} e^{-\beta\epsilon_{n'}} f(\epsilon_n - \epsilon_{n'}) \times (\delta_{\nu\hat{\nu}}A_{nn';nn'} - \langle n|J^{-\nu}|n'\rangle \times \langle n'|J^{\hat{\nu}}|n\rangle) + \Delta_{s\ell}\delta_{\nu\hat{\nu}} \,, \tag{9a}$$

$$\Delta_{\nu,\hat{\alpha}\hat{\alpha}'} = 8\pi J_{sf}^2\rho_0\frac{c\beta}{Z}e^{-\beta\epsilon_{\hat{\alpha}}}\sum_n f(\epsilon_n - \epsilon_{\hat{\alpha}})B^{\nu}_{n;\hat{\alpha}\hat{\alpha}'} \,, \tag{9b}$$

$$\Delta_{\alpha\alpha',\hat{\nu}} = 4\pi J_{sf}^2\rho_0^2\sum_n f(\epsilon_n - \epsilon_\alpha)B^{-\hat{\nu}}_{n;\alpha'\alpha} \,, \tag{9c}$$

$$\Delta_{\alpha\alpha',\hat{\alpha}\hat{\alpha}'} = 2\pi J_{sf}^2\rho_0^2\Big(\delta_{\alpha'\hat{\alpha}'}\sum_n A_{n\hat{\alpha};n\alpha}f(\epsilon_n - \epsilon_\alpha) + \delta_{\alpha\hat{\alpha}}\sum_n A_{\hat{\alpha}'n;\alpha'n}f(\epsilon_n - \epsilon_\alpha) - 2A_{\alpha\hat{\alpha};\alpha'\hat{\alpha}'}f(\epsilon_{\hat{\alpha}} - \epsilon_\alpha)\Big) \,, \tag{9d}$$

where $f(x) = x(e^{\beta x} - 1)^{-1}$ and where we have introduced the quantities

$$A_{n_1n_2;n_3n_4} = \sum_\nu \langle n_1|J^\nu|n_2\rangle\langle n_4|J^{-\nu}|n_3\rangle \,, \tag{10}$$

and

$$B^1_{n;\alpha\alpha'} = (B^{-1}_{n;\alpha'\alpha})^* = \langle n|J^{-1}|\alpha\rangle\langle\alpha'|J^0|n\rangle - \langle n|J^0|\alpha\rangle\langle\alpha'|J^{-1}|n\rangle \,, \tag{11a}$$

$$B^0_{n;\alpha\alpha'} = \langle n|J^1|\alpha\rangle\langle\alpha'|J^{-1}|n\rangle - \langle n|J^{-1}|\alpha\rangle\langle\alpha'|J^1|n\rangle \,. \tag{11b}$$

The matrix $\Delta_{M\hat{M}}$ describes the relaxation between the individual subsystems, while the fields seen by these systems are described by the remaining part of $\Omega_{M\hat{M}}$. The conduction-electron–lattice relaxation rate $\Delta_{s\ell}$, not specified in our theory, is retained as a phenomenological parameter. $\Delta_{1,1} = \Delta_{-1,-1}$ and Δ_{00} are, apart from $\Delta_{s\ell}$, the transverse and the longitudinal Overhauser rates,[5,15] generalized to allow for the presence of the crystal field. The diagonal terms $\Delta_{\alpha\alpha',\alpha\alpha'}$ in Eq. (9d) represent the Korringa relaxation rates for the individual crystal-field transitions, as obtained previously.[4] The off-diagonal terms of Eq. (9) represent the "scattering in"[10] relaxation rates and have not been obtained previously for this problem.

We would like to mention that, as in the S-state problem, Eq. (9) contains the detailed balance relations

$$\Delta^*_{M\hat{M}}/\Delta_{\hat{M}M} = \chi^0_{\hat{M}}/\chi^0_M \,.$$

In our approximation, $\chi_{M\hat{M}}$ remains a positive definite Hermitian matrix, $L_{M\hat{M}}$ remains a Hermitian matrix and $\chi^0_M\Delta_{M\hat{M}}$ a positive semidefinite matrix. Therefore the matrix $\omega\,\mathrm{Im}\chi^{\nu\nu'}(\omega)$ is in our approximation negative semidefinite, which guarantees positive energy absorbtion.

The coupled resonance equations, as given in this section, describe both the ESR and CESR spectra of localized moments dissolved in a metal. Since the crystal field is arbitrary in these equations, many different physical situations are included once the crystal field is specified. In general, the full solution of these equations can only be found by computer calculations. However, the qualitative behavior of the solutions can be discussed in several limiting cases, as was done for the S-state problem,[7,8,10] to which the reader is referred for more details. If all the widths Δ and all the internal fields are small compared to all the differences of the bare resonance frequencies $g_s\mu_B H$ and $g_J\mu_B H(\langle\alpha|J^0|\alpha\rangle - \langle\alpha'|J^0|\alpha'\rangle)$ then all the resonances are uncoupled. Their resonance frequencies and widths are given by the real and imaginary parts of the diagonal elements of $-\Omega_{MM}(\omega=0)/\chi_{MM}$, respectively. Their oscillator strengths are given in this case by the corresponding $(e^\nu_M)^*\chi_{MM}e^{\nu'}_M$. If, however, two or more bare transition frequencies are close together in frequency (compared to their widths and the internal fields), then the coupling cannot be neglected. Narrowing effects will occur in the lines involved, as previously discussed[7,8,10] and seen experimentally[9,10] for S-state ions.[16]

To conclude this general discussion, we would like to point out that in many practical cases the equations can be simplified. The overall zero-

field splitting is typically several hundred degrees, so the temperature is usually much smaller than the energy of the higher crystal-field multiplets. For transitions within the higher crystal-field multiplets, the Boltzmann factor becomes extremely small. An analysis of our equations shows that these transitions then have only a negligible influence on the spectrum. This reduces the dimension of the transition matrix and simplifies the numerical calculations.

III. DISCUSSION OF A PHYSICAL EXAMPLE

As pointed out in the last section, our equations contain, in principle, the same limiting cases as the S-state problem. We do not give, therefore, a complete treatment of all the cases. We will, however, discuss in some detail a particular example, with physically reasonable parameters, which shows some interesting features resulting from the coupling.

We choose a crystal field with cubic symmetry and describe it by the usual crystal field Hamiltonian[17]

$$H_c = W\left[x\left(\frac{O_4}{F(4)}\right) + (1-|x|)\left(\frac{O_6}{F(6)}\right)\right]. \tag{12}$$

The parameters W and x, defined in Ref. 17, can be estimated from experimental data.[5,18] With a choice of these values, the full multiplet structure is determined. We shall restrict ourselves further to the case of a Γ_7 doublet ground state and a Γ_8 quartet first excited state at an energy δ above the ground state, as shown in Fig. 1. For a given x, the choice of δ fixes W. All other excited levels are assumed to be much higher, so that they do not influence the spectra up to temperatures of the order of δ. We have chosen to align the magnetic field with the [100] direction. Due to the special symmetry and to time reversal the transverse susceptibility is given by $\chi^{11}(\omega)+[\chi^{11}(-\omega)]^*$. Again due to the symmetry e^1_M is nonvanishing only for $M=\nu=1$ (representing $\langle s^1\rangle$) and for five crystal-field transitions,[19] one within the Γ_7 and four within the Γ_8 (Fig. 1). A straightforward calculation, using the cubic symmetry, shows that these five transitions and $\langle s^1\rangle$ do not couple to the remaining crystal-field transitions or to $\langle s^0\rangle$ and $\langle s^{-1}\rangle$. Thus, we can work with a 6×6 transition matrix, which simplifies the numerical calculation. We choose $J=\frac{15}{2}$ and $x=0.4$, which leads to effective g factors of 7.55 for the Γ_7 and of -4.34, -8.71 and 6.53 (twice) for the Γ_8 transitions. Since the results given in Sec. II are limited to temperatures large compared to the transition energies, we have considered magnetic field strengths appropriate for CESR or ESR at 10 GHz and limited the temperature range of the graphs accordingly.

We characterize the host material by its conduction-electron g value, 2, its density of states, $\rho_0=0.2$ states/(eV spin atom), and a temperature independent contribution to Δ_{sl}, equal to 3.5×10^8 sec^{-1}. The host-local moment interaction is specified by $J_{sf}=0.033$ eV and a concentration dependent contribution to Δ_{sl}, equal to 5×10^{11} sec^{-1}/(atomic percent of impurity). The parameters chosen for our example may be reasonable for Dy or Er in a noble-metal or aluminum host.[2,5] However, it is not the aim of this paper to give an analysis of any particular experiment, since our knowledge of the data is not sufficient to allow this.

To obtain the shifts and widths of the spectra, we have calculated, by computer, the roots of the transition matrix $\Omega_{MM'}$. We have done this calculation for two different values of the splitting δ, 200 K and 40 K, and for two different local moment concentrations, 20 and 2000 ppm (atomic). For both values of δ and over the whole temperature range from 2 to 50 K, only two lines have reasonably small widths and reasonably large oscillator strengths simultaneously. One of these roots has basically conduction-electron character (referred to as the CESR line), and the other has basically Γ_7 ground-state character (called the ESR line). Although the transitions within the Γ_8 quartet cannot be seen in the spectrum,[20] the coupling of these transitions to the conduction electrons and the Γ_7 has important consequences for the CESR and ESR lines. The results of the computer calculations are given in Figs. 2–9.

To make the effects due to the coupling clearer, the dotted (20 ppm) and dash-dot (2000 ppm) lines in each figure show the behavior when the coupling of the transitions is neglected. These lines show the Knight and "Day" shifts, and the Korringa and Overhauser rates for the ESR and CESR lines, respectively, in the presence of the crystal field.

A. Crystal-field splitting δ = 200 K

In this case the coupling with the Γ_8 resonances can be neglected in practice over the whole temperature range shown. Thus only the coupling of the ESR and CESR lines remains. All the behavior of the shifts and widths can be understood in terms of the general behavior of two coupled resonances. "Turning on" the coupling of two originally well separated and uncoupled oscillators results in a pulling together of their resonance frequencies. The resonance with the originally smaller width will be narrowed, and the originally broader line will be broadened by "turning on" the coupling. In the language of Refs. 9 and 10, this represents the onset of narrowing.

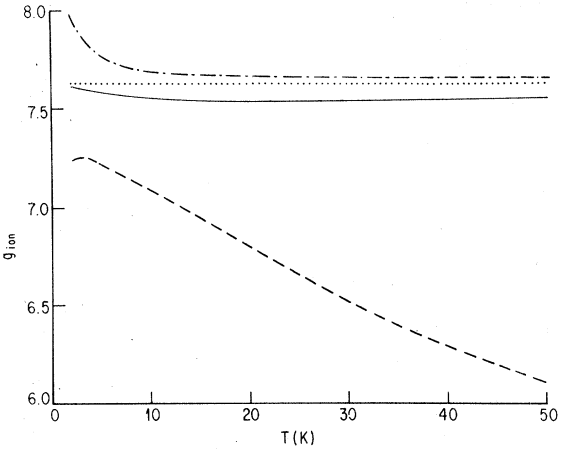

FIG. 2. Ionic g value as a function of temperature for multiplet splitting $\delta = 200$ K. The resonance frequency displays a shift even in the absence of coupling (Knight shift). In this and the following figures, the dotted line refers to the 20-ppm concentration and the dash-dot line to the 2000-ppm concentration, respectively, in the absence of coupling. The exact results are shown by a solid line for 20 ppm and a dashed line for 2000 ppm.

These general features can clearly be seen in Figs. 2–5. The ESR g value (Fig. 2) is decreased with increasing concentration, while the CESR g value (Fig. 3) is increased, relative to the corresponding uncoupled values (dotted and dash-dot lines). [Note that in Fig. 3 $(\omega - \omega_s)/c$ is plotted, so that the 2000-ppm shift is actually much greater than the 20-ppm shift.] For 20 ppm, the Overhauser rate is smaller than the Korringa rate. As seen in Fig. 5, the CESR width becomes smaller than the Overhauser rate. The ESR width is

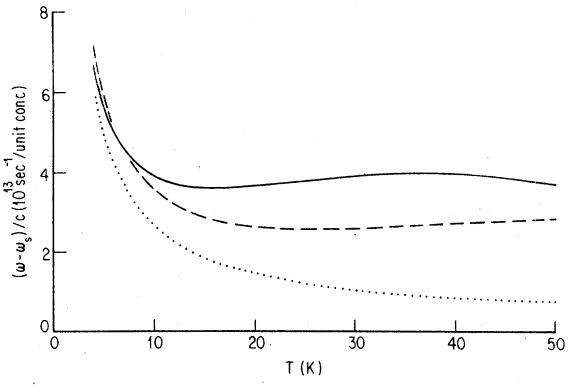

FIG. 3. Shift of the conduction-electron frequency relative to $\omega_s = g_s \mu_B H$ for $\delta = 200$ K. Note that in the uncoupled case, the shift is approximately proportional to impurity concentration ("Day" shift), and that all shifts have been divided by the fractional concentration. As plotted, the uncoupled shifts are nearly coincident, so only one line is shown.

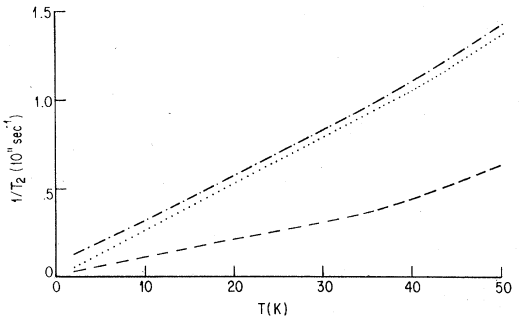

FIG. 4. Transverse relaxation rate of the local moment as a function of temperature for $\delta = 200$ K. The 20-ppm exact result is only slightly above the 20-ppm uncoupled result (Korringa rate), so only one line is shown.

larger than the Korringa rate, although this increase cannot be seen on the scale of Fig. 4. For 2000 ppm, however, the Overhauser rate is larger than the Korringa rate. Thus, the CESR line is broadened (Fig. 5) and the ESR line is narrowed (Fig. 4).

B. Crystal-field splitting $\delta = 40$ K

It is clear that for temperatures below about 10 K, the behavior of the lines is qualitatively similar to that seen for large splitting. At higher temperatures the coupling to the Γ_8 resonances plays an important role. Thus, we have to treat six coupled equations for our simple example, and a straightforward explanation of the effects occurring seems to be difficult. However, the general pulling together of the resonance positions, or onset of the narrowing, can again be clearly seen in Figs. 6 and 7. The ESR line width is now smaller than the Korringa width for both

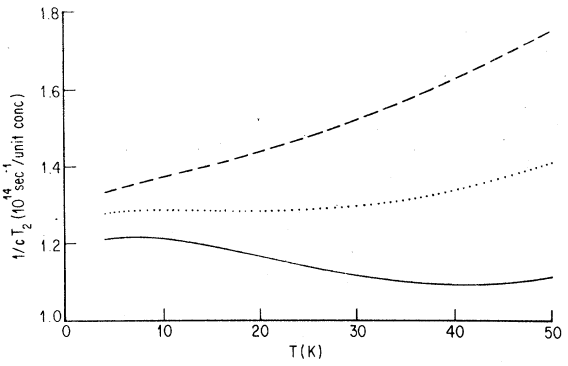

FIG. 5. Transverse relaxation rate of the conduction electrons as a function of temperature for $\delta = 200$ K. Since the uncoupled rate (Overhauser rate) is exactly proportional to the concentration, all the rates have been divided by the concentration, and only one line is shown for the uncoupled rates.

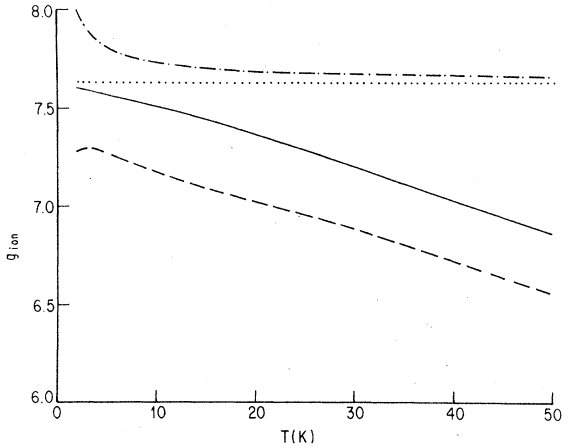

FIG. 6. Ionic g value as a function of temperature for multiplet splitting $\delta = 40$ K.

concentrations (Fig. 8). (The Korringa width is nonlinear in temperature due to the presence of the Γ_8 levels.[4]) The CESR line is narrowed for the low concentration, but broadened for the high concentrations (Fig. 9).

IV. SUMMARY AND CONCLUSIONS

We have presented a description of the full dynamics of localized moments dissolved in a metal, in the presence of a crystal field. The crystal-field scheme is completely general, so that our results describe a large variety of physical situations. In particular, all non-S-state ions are included for the first time. In agreement with the actual physical situation, we have restricted our

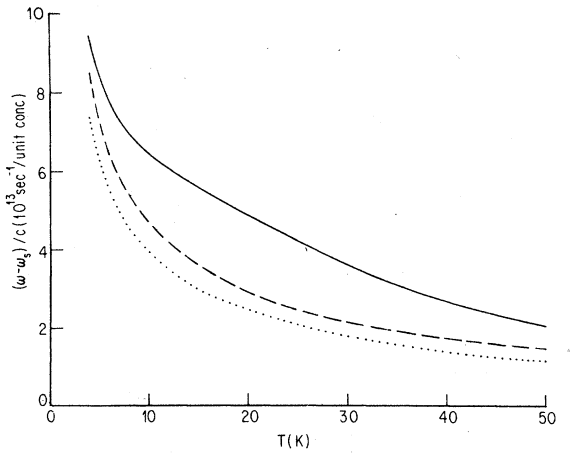

FIG. 7. Shift of the conduction-electron frequency relative to $\omega_s = g_s \mu_B H$ for $\delta = 40$ K. Below 20 K, the normalized shift of the uncoupled 2000-ppm result is slightly greater than that of the uncoupled 20-ppm result, but the difference is too small to show.

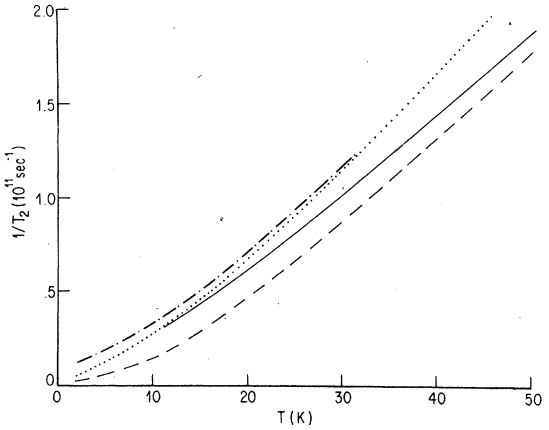

FIG. 8. Transverse relaxation rate of the local moment as a function of temperature for $\delta = 40$ K. Where lines merge, below 10 K or above 35 K, only one line is shown.

treatment to temperatures large compared to the Zeeman splittings.

We have shown, for a physically reasonable example, that even when the resonance frequency of the conduction electrons and the resonance frequency of a doublet ground state are very different ($g_s = 2$, $g_{ion} = 7.55$), the coupling between the conduction electrons and the local moments can become important. This coupling can lead to a decrease of the thermal slope of the ESR linewidth with increasing local moment concentration and to a large temperature-dependent g shift of the local moment ground-state resonance. The decrease of the ESR linewidth slope at low temperature is extremely interesting, since the measured slope of the actual ESR spectrum may not be the Korringa slope. The measured slope is often used to deduce the exchange parameter[2] J_{sf} which may be

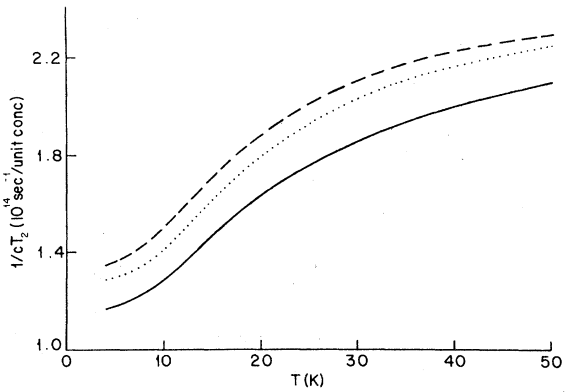

FIG. 9. Transverse relaxation rate of the conduction electrons as a function of temperature for $\delta = 40$ K. As in Fig. 5, only one line is shown for the uncoupled rates.

in error if the possible coupling due to a large Overhauser rate is not considered. Our example also shows that the CESR shift does not follow the local moment susceptibility if significant coupling is present due to a large Korringa rate and/or the proximity of an excited state. This behavior is important when using the conduction-electron g shift to obtain information about the crystal-field structure of the local moments.[5]

Finally, we should consider whether or not any of the effects discussed here could be studied in a systematic way. As noted above, the parameters chosen for calculation are reasonable for Dy or Er in a noble-metal or aluminum host. ESR experiments could be done in such a system, over the indicated concentration range. The measurements would probably be limited to low temperatures, since, for the parameters chosen here, the ESR linewidth is comparable to the resonant frequency at about 15 K. It should still be possible to see some of the concentration dependences, even within the low-temperature range. In fact, a concentration dependence of the linewidth has been observed in Cu:Er,[21] although no g shift was reported. CESR measurements could be performed over the entire temperature range, but line broadening due to the rare-earth impurity will probably limit experiments to low concentrations. This will limit the study of concentration effects, but it should be possible, in a favorable case, to observe a CESR g shift which does not decrease as sharply with temperature as the single-ion susceptibility.

ACKNOWLEDGMENTS

We wish to acknowledge interesting and informative discussions with R. L. Orbach and J. F. Siebert. This work was supported by the NSF under Grant No. DMR 75-19544 and by the Office of Naval Research under Contract No. N00014-75-C-0245. Computer time was supplied by a grant from the UCLA Campus Computing Network. One of the authors (T.P.) wishes to thank the "Sonderforschungsbereich Festkörperspektroskopie Darmstadt-Frankfurt," a special fund of the Deutsche Forschungsgemeinschaft, for generous support.

---

*Present address: Dept. of Physics, Rice University, Houston, Texas 77001.
†Permanent address: Lehrstuhl für Theoretische Festkörperphysik, Technische Hochschule Darmstadt, Darmstadt, West Germany.

[1]R. Orbach, M. Peter, and D. Shaltiel, Arch. Sc. Genéve 27, 141 (1974).
[2]R. H. Taylor, Adv. Phys. 24, 681 (1975).
[3]H. Hasegawa, Prog. Theor. Phys. (Kyoto) 21, 483 (1959).
[4]L. L. Hirst, Phys. Rev. 181, 597 (1969).
[5]J. F. Siebert, S. A. Dodds, and R. H. Silsbee, Phys. Rev. B 14, 4813 (1976).
[6]A typical value is 10^{11} $\sec^{-1}$ or 3000 G for a concentration of 1000 ppm. In an applied field of 1000 G, this would require a difference in g values of about 10 to avoid overlap.
[7]S. E. Barnes, Phys. Rev. B 9, 4789 (1974).
[8]T. Plefka, Phys. Status Solidi B 51, K113 (1972); 55, 129 (1973).
[9]J. M. Moret, R. Orbach, M. Peter, D. Shaltiel, J. T. Suss, W. Zingg, and R. A. B. Devine, Phys. Rev. B 11, 2002 (1975); P. Urban, D. Davidov, B. Elschner, T. Plefka, and G. Sperlich, Phys. Rev. B 12, 72 (1975).
[10]P. H. Zimmerman, D. Davidov, R. Orbach, L. J. Tao, and J. Zitkova, Phys. Rev. B 6, 2783 (1972).
[11]In principle, still more Bloch equations are needed for the transitions between two different multiplets. However, the latter equations will, to a good approximation, decouple from our set due to the high frequency of the transitions involved.
[12]H. Mori, Prog. Theor. Phys. (Kyoto) 34, 399 (1965).
[13]The projector P onto the subspace of the Liouville space is spanned in our problem in a natural way by the components of the conduction-electron magnetization and all the crystal-field transition operators $|\alpha\rangle\langle\alpha'|$.
[14]As in Ref. 8, we neglect the frequency dependence of the self-energy, which is a good approximation at high temperature.
[15]Reference 5 gives the longitudinal rate, which agrees with the transverse rate for special symmetries.
[16]The narrowing effects for non-S-state ions are not expected to be as drastic as for S-state ions. For S-state ions, all the resonance frequencies become approximately equal at a particular field angle, leading to a collapse of the spectrum. This situation is unlikely to occur for non-S-state ions.
[17]K. R. Lea, M. J. M. Leask, and W. P. Wolf, J. Phys. Chem. Solids 23, 1381 (1962).
[18]G. Williams and L. L. Hirst, Phys. Rev. 185, 407 (1969).
[19]A. Abragam and B. Bleaney, *Electron Paramagnetic Resonance of Transition Ions* (Oxford University, London, 1970).
[20]Transitions within the Γ_8 quartet have small oscillator strengths at low temperatures due to the Boltzmann factor. These transitions might be seen at higher temperatures in some cases. For our choice of parameters, the high-temperature widths are too large to allow experimental observation.
[21]T. S. Al'tshuler, M. M. Zaripov, E. F. Kukovitskii, E. P. Khaimovich, and E. G. Kharakhash'yan, Pis'ma Zh. Eksp. Teor. Fiz. 20, 416 (1974) [JETP Lett. 20, 187 (1974)].